Supplementary Material (ESI) for Analytical Methods

Electronic supplementary material

Ring magnets for magnetic beads trapping in a capillary

Anne-Laure Gassner[1], Jacques Morandini[2], Jacques Josserand[1], and Hubert H. Girault[1]*

[1]Laboratoire d'Electrochimie Physique et Analytique, EPFL SB ISIC LEPA, Lausanne, Switzerland

[2]Astek Rhone-Alpes, 1 place du Verseau, 38130 Echirolles, France

Correspondence:

Professor Hubert H. Girault, Ecole Polytechnique Fédérale de Lausanne, Laboratoire d'Electrochimie Physique et Analytique, EPFL SB ISIC LEPA, Station 6, CH-1015 Lausanne, Switzerland

E-mail: hubert.girault@epfl.ch

Tel: +41 21 6933145

Fax: +41 21 6933667

SI 1: Finite-element formulation of the magnetic field

The integral formulation is based on the local form given by Eq (1) using the scalar potential ϕ:

$$div\boldsymbol{B} = \nabla \bullet \left(-\mu \nabla \phi + \boldsymbol{B_0}\right) = 0 \qquad \text{(S1)}$$

Equation (S1) is derived in the global form (S2), using the Galerkin formulation frequently used in the finite element method (multiplication by a projective function α and integration on the domain of study).

$$\iint \left[\alpha \nabla \bullet \left(-\mu \nabla \phi + \boldsymbol{B_0}\right)\right] d\omega = 0 \qquad \text{(S2)}$$

By decomposing the product between α and the divergence in (S2), the second order derivative of the unknown ϕ (divergence of $\nabla\phi$) becomes:

$$\alpha \nabla \bullet (-\mu \nabla \phi + \boldsymbol{B_0}) = \nabla \bullet \left[\alpha\left(-\mu \nabla \phi + \boldsymbol{B_0}\right)\right] - \nabla \alpha \bullet \left(-\mu \nabla \phi + \boldsymbol{B_0}\right) \qquad \text{(S3)}$$

Equation (S3) is applied in (S2) and the Ostrogradsky theorem is used to reject the divergence term $\nabla \bullet \left[\alpha\left(-\mu \nabla \phi + \boldsymbol{B_0}\right)\right]$ at the boundary in (S4) where it equals to zero (no magnetic field at the external boundaries of the domain due to the use of a large "air box").

$$\iint \left[\nabla \alpha \bullet \left(\mu \nabla \phi - \boldsymbol{B_0}\right)\right] d\omega + \int \alpha \boldsymbol{B} \bullet n \, d\omega = 0 \qquad \text{(S4)}$$

The unknown vector ϕ is interpolated with a function β, of the same type as the projective function α as the Galerkin method is used. It leads to the final form (S5) where the first term corresponds to the matrix to invert, the second term being the source term (discretization non described).

$$\iint \mu \nabla \alpha \bullet \nabla \beta \, \phi \, d\omega = \iint \nabla \alpha \bullet \boldsymbol{B_0} \, d\omega \qquad \text{(S5)}$$

***SI 2*: Finite-element formulation of the species concentration**

The local form (7) is written in the global form (S6), using the Galerkin formulation.

$$\iint \alpha \left[\frac{\partial c}{\partial t} + div\left(-D\nabla c + (\boldsymbol{v}_{flow} + \boldsymbol{v}_{mag})c \right) \right] d\omega = 0 \qquad \text{(S6)}$$

Using the $\boldsymbol{v}_{\mathrm{mag}}$ expression given by (6), we obtain :

$$\iint \alpha \left[\frac{\partial c}{\partial t} + \nabla \bullet \left(-D\nabla c + \boldsymbol{v}_{flow} c + \frac{\boldsymbol{F}_{mag}}{6\pi\eta r} c \right) \right] d\omega = 0 \qquad \text{(S7)}$$

By decomposing the product between α and the divergence for the diffusion term, the second order derivative of the concentration (divergence of the gradient ∇c) becomes:

$$\alpha \nabla \bullet (-D\nabla c) = \nabla \bullet (-\alpha D\nabla c) + D\,\nabla\alpha \bullet \nabla c \qquad \text{(S8)}$$

(S8) is injected in (S7). Using the Ostrogradsky theorem, the divergence term $\nabla \bullet (-\alpha D\nabla c)$ is rejected at the boundary in (S11), where it expresses the diffusion flux boundary condition. In the present case of study, it equals to zero (no flux across the boundaries of the domain). The convection term in (S7) is derived by taking into account the continuity equation $\nabla \bullet \mathrm{v}_{flow} = 0$.

$$\nabla \bullet \left(\boldsymbol{v}_{flow} c \right) = \boldsymbol{v}_{flow} \nabla c + c \nabla \bullet \boldsymbol{v}_{flow} = \boldsymbol{v}_{flow} \nabla c \qquad \text{(S9)}$$

The magnetic term in (S7) can't be treated in the same way, as the magnetic force and velocity are not conservative ($\nabla \bullet \mathrm{v}_{mag} \neq 0$). Consequently, this term is derived as the diffusion one by decomposing the product between α and the divergence:

$$\alpha \nabla \bullet \left(\frac{\boldsymbol{F}_{mag}}{6\pi\eta r} c \right) = \nabla \bullet \left(\alpha \frac{\boldsymbol{F}_{mag}}{6\pi\eta r} c \right) - \nabla\alpha \bullet \frac{\boldsymbol{F}_{mag}}{6\pi\eta r} c \qquad \text{(S10)}$$

Applying (S10) in (S7) and using the Ostrogradsky theorem, the divergence term is rejected at the boundary, where it equals to zero (no magnetic force at the boundaries of the domain). Consequently, only the surface integral of (S11) is conserved in (S12).

$$\iint \left[\alpha \frac{\partial c}{\partial t} + D\nabla\alpha \bullet \nabla c + \alpha \boldsymbol{v}_{flow} \nabla c - \frac{c}{6\pi\eta r} \nabla\alpha \bullet \boldsymbol{F}_{mag} \right] d\omega + \int \alpha \left[-D\nabla c \bullet n + \frac{c}{6\pi\eta r} \boldsymbol{F}_{mag} \bullet n \right] d\omega = 0$$

(S11)

Using the β function for the interpolation of the unknown vector *c*, the final form is obtained (discretization non described).

$$\iint \left[\alpha \frac{\partial c}{\partial t} + \left(D\nabla\alpha \bullet \nabla\beta + \boldsymbol{v}_{flow} \alpha \nabla\beta - \frac{1}{6\pi\eta r} \beta \nabla\alpha \bullet \boldsymbol{F}_{mag} \right) c \right] d\omega = 0 \qquad \text{(S12)}$$

SI 3: Immunoassay protocol

As presented by Chen *et al*., the procedure is composed of 6 steps. The pressures and times were adapted to the present case. The goal of this experiment was not to carry out quantitative measurements, but just to show the influence of the pressure on the results with exactly the same protocol. Increasing the pressure gives the opportunity to decrease rinsing times and even loading times for antibody and antigen, reducing the assay time.

Step 1: **MBs trapping** → a uniform suspension of MBs is injected into the capillary for 1 min at 2 psi (138 mbar).

Step 2: **Antibody immobilization** → anti-β-LG antibodies (100 µg/mL) are injected for 10 min at 1, 2 or 5 psi.

Step 3: **Antigen immunocapture** → β-LG (100 µg/mL) is injected for 5 min at 1, 2 or 5 psi.

Step 4: **Washing** → the binding buffer is injected at 1, 2 or 5 psi for 10, 5 and 2 min respectively to remove unbound proteins and totally fill the capillary. This binding buffer is used as the leading buffer for ITP stacking.

Step 5: **Reverse rinsing** → a plug of separation buffer was injected at 34.5 mbar from the outlet vial for 3 min.

Step 6: **Release and separation of the antigens and antibodies** → 15 kV are applied from anode to cathode with electrode compartments filled with separation buffer. As electrophoresis occurs, the pH in the zone of MBs gradually diminishes until a value where the immunocomplexes are dissociated. The antigen and the antibody are then released from the MBs, stacked by t-ITP and finally separated by CZE.

SI 4: Description of the Plexiglas holder for MBs plugs imaging

As it is not possible to image MBs plugs with drilled cylindrical magnets, rectangular ones (5x5x1 mm^3) were placed on each side of the capillary (75/375 µm i.d./o.d.) to enable the visualization of MBs accumulation. The permanent magnets were introduced in a Plexiglas holder, which is a rectangular plate of Plexiglas (2.5 cm large, 7.5 cm long and 5 mm thick) in which holes for the magnets were dug. Figure S1 shows a scheme of the holder, with the Plexiglas part in blue grey, the capillary in orange and the magnets in grey.

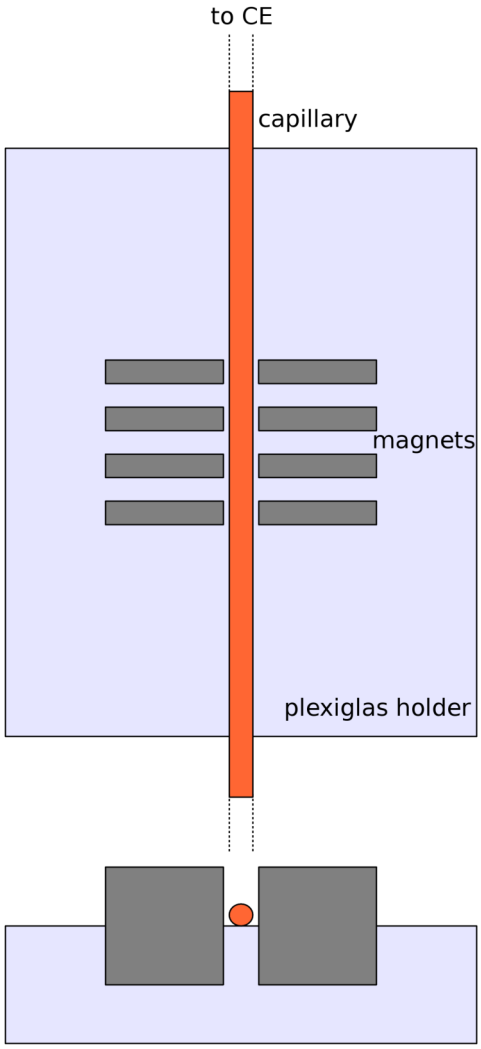

Figure S 1: Plexiglas holder, with on top: view from the top and on the bottom: section view. Magnets are in grey, capillary in orange and Plexiglas in blue grey.

Half of the magnets' height is inserted into the holder, such as the capillary is more or less in the middle of the magnets' height. The capillary is placed symmetrically between the two magnets columns and is connected to the CE, which is used in pressure mode to flow the solutions through the capillary. The exit of the capillary is located just after the end of the Plexiglas holder and is not connected to anything. The total length of the capillary is 1 m.

SI 5: Parametric study with one magnet

As mentioned in the text, the influence of the magnet internal radius $r_{mag.int}$ was studied. Fig. S2 reminds of the parameters presented in the article.

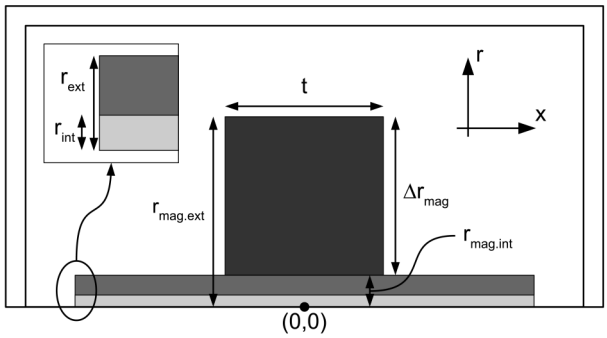

Figure S 2: Scheme of the system composed of a capillary with internal radius r_{int} and external radius r_{ext} surrounded by one permanent magnet (dark grey) defined by the difference between its external and internal radius Δr_{mag} and its thickness t. The area between the two external double lines represents the infinite air box. d is the thickness of the spacer.

Fig. S3 presents the effect of the magnet internal radius $r_{mag.int}$ for a single magnet. Its value was varied from the external radius of the capillary r_{ext} (187.5 µm, magnet in contact with the capillary) to 1000 µm, keeping Δr_{mag} and t constant (2 mm).

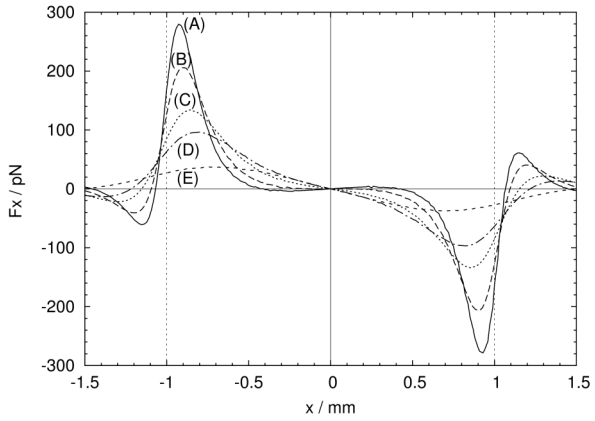

Figure S 3: Variation of the magnetic force (x component) for a single magnet in function of the internal radius of the magnet $r_{mag.int}$ ($\Delta r_{mag} = t = 2$ mm). $r_{mag.int}$ equal to: (A) 187.5 µm, (B) 250 µm, (C) 375 µm, (D) 500 µm and (E) 1000 µm. The forces were calculated for a bead of radius = 500 nm and $B_0 = 1$ T. All the values are taken along the x-axis. The vertical dashed lines show the magnet position.

As for rectangular magnets with a magnetization perpendicular to the microchannel, two magnetic force peaks (positive and negative) are obtained inside the magnet borders, generating a plug in the magnet centre. It can also be seen that the magnetic force decreases rapidly when $r_{mag.int}$ increases. This is due to the gradient in the $(\boldsymbol{B}\bullet\nabla)\boldsymbol{B}$ term (see Eq. 3), which is induced by the rotation of the magnetic field lines around the magnet. The less space they have at their disposal to turn, the higher will be the gradient. When $r_{mag.int}$ increases, they have more space to turn and they enlarge, decreasing the local gradient. Moreover, the magnetic flux density decreases with the distance. The

isovalues of Figure S4 shows the distribution of ***B*** for r_{ext} of 375 and 1000 µm respectively. Note that, contrary to the previous figure, the horizontal axis is the *r*-axis and the vertical axis is the *x*-axis.

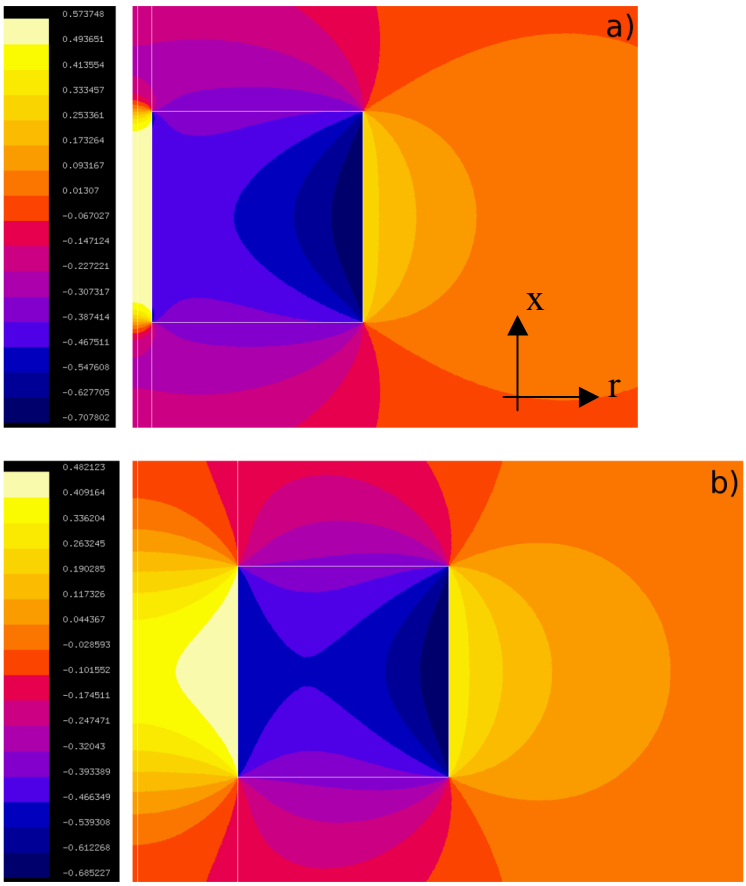

*Figure S 4: Isovalue representation of the x component of the magnetic flux density **B** for r_{ext}: a) 187.5 µm and b) 1000 µm. $\boldsymbol{B_0}$ = 1T, Δr_{mag}= t = 2mm*

The scale on the left shows that the magnetic flux density is higher when the magnet is near the capillary. Indeed when the field lines have to pass through a thin space, they are more confined, increasing the local ***B*** value. The same explanation is true for the gradient. Magnetic lines are forced to turn on a short distance, creating a high gradient when the magnet is near the capillary. The magnetic force being dependent on both ***B*** and its local gradient, it is consequently higher when the magnet is in contact with the capillary. As a consequence, $r_{mag.int}$ should be as small as possible to maximize the force, leading to the use of a magnet with a hole diameter of a size equal to the capillary outer diameter.

As mentioned in the paper, Figure S5 presents magnetic flux isovalues corresponding to $\Delta r_{mag}/t$ ratios of 1 and 5 respectively. The left scale shows clearly that a higher local $\boldsymbol{B}$ (around 50 % increase) is obtained when the magnet is flat as a disc, the gradient of $\boldsymbol{B}$ remaining similar. This is due to the magnetic lines having a longer way to go if they go round the magnet, such as more lines pass through the capillary.

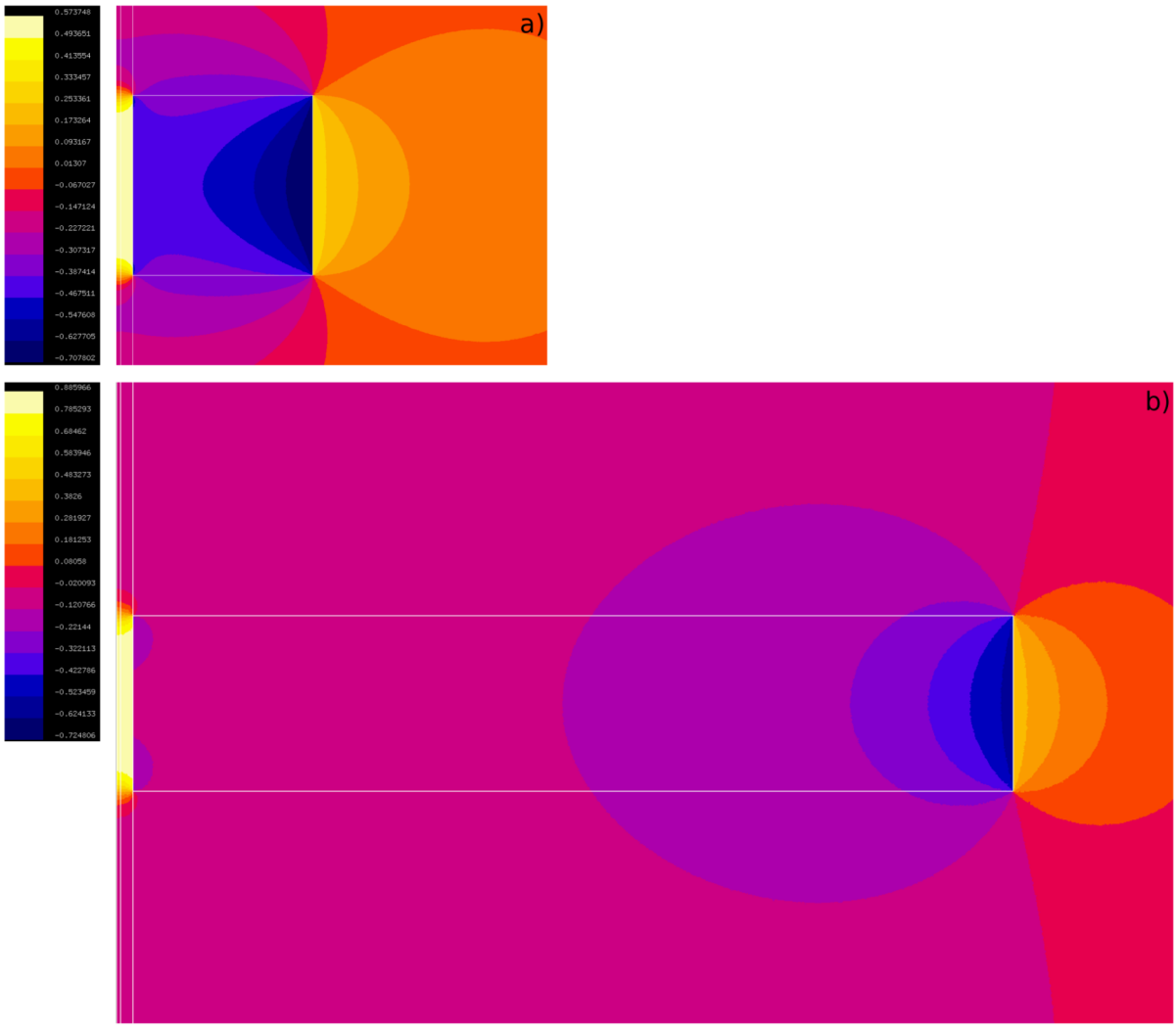

Figure S 5: Isovalue representation of the x component of the magnetic flux density $\boldsymbol{B}$ *for a)* $\Delta r_{mag}/t$*: 1 and b)* $\Delta r_{mag}/t$*: 5.* $\boldsymbol{B_0}$ *= 1T, t = 2 mm and* r_{ext} *= 187.5 µm*

In conclusion, for a ring magnet, the highest magnetic force is obtained for a flat disk magnet, with a "radius" Δr_{mag} larger than its thickness, and this magnet has to be in close contact with the capillary (small hole).

SI 6: Four magnets system (thickness of the spacers)

The interaction of four magnets is now considered. Disk magnets with a small hole are used. The following parameters are used: $r_{mag.int}$ = 187.5 µm, Δr_{mag} = 5 mm and t = 1 mm. The four magnets can be arranged in two opposite configurations: attraction and repulsion. In attraction, the magnetization of all the magnets points in the same direction (NS-NS-NS-NS), whereas in repulsion, the magnetization alternates (NS-SN-NS-SN). Different spacer thicknesses d, from 0.5 mm to 4 mm, were simulated in order to study their influence on the magnetic force.

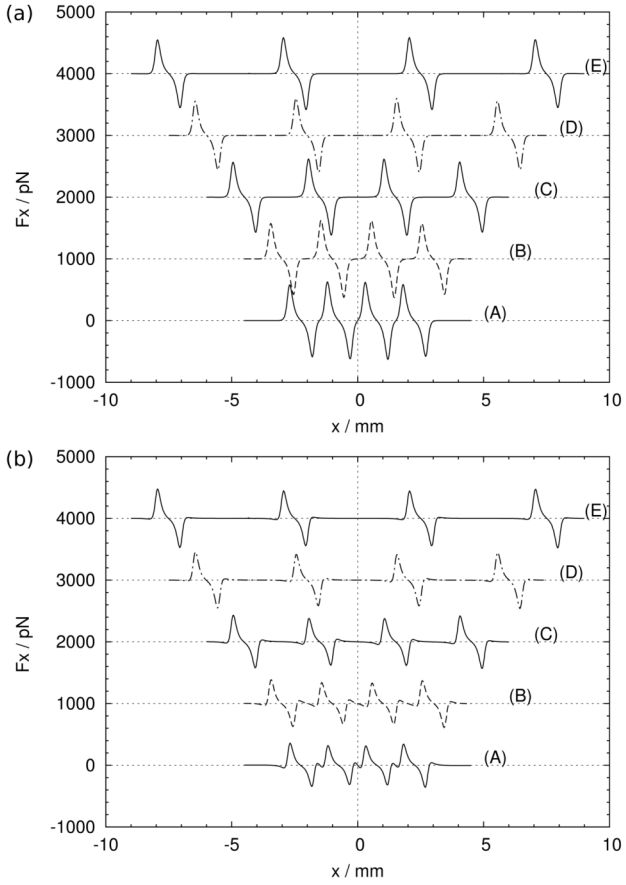

Figure S 6: Variation of the magnetic force (x component) for four magnets in (a) repulsion and (b) attraction, for different spacer thicknesses d. (A) 0.5 mm, (B) 1 mm, (C) 2 mm, (D) 3 mm and (E) 4 mm. The forces were calculated for a bead of radius = 500 nm and B_0 = 1 T. $r_{mag.int}$ = 187.5 µm, Δr_{mag} = 5 mm and t = 1 mm. All the values are taken along the x-axis. The curves were shifted vertically for clarity and the horizontal dashed lines show the zero for each curve..

As shown by Fig. S6a, four MBs plugs may be formed in repulsion, more precisely one in the middle of each magnet. The parameter d has no effect on the shape of the curves, but for a d value of 0.5 mm, the maximum force is around 7% higher than for 4 mm. This is due to the opposing magnetic fields, which have to turn in a very reduced space when d is small, increasing the $\boldsymbol{B}$ gradient. In attraction, the number of possible plugs is dependent on d. For large spacer thicknesses,

four plugs are formed like in repulsion, whereas for small *d*, three additional inter-magnet plugs with a smaller force are added. In contrast to repulsion, largest ***F*** values are obtained with large spacer thicknesses (around 37% increase between 0.5 and 4 mm). This effect is due to the bigger space given to the magnetic field lines to enlarge between the magnets for large *d* values. The comparison of repulsion and attraction cases shows that the magnetic force is larger in repulsion in all the *d* cases, from 21% when *d* is equal to 4 mm to 77% for a *d* value of 0.5 mm. In order to minimize the distance between MBs plugs and to be experimentally feasible, a spacer thickness of 1 mm was chosen for the rest of the study.

For information, magnetic flux density isovalues (x component, vertical axis) are showed in Figure S7, in repulsion and attraction respectively.

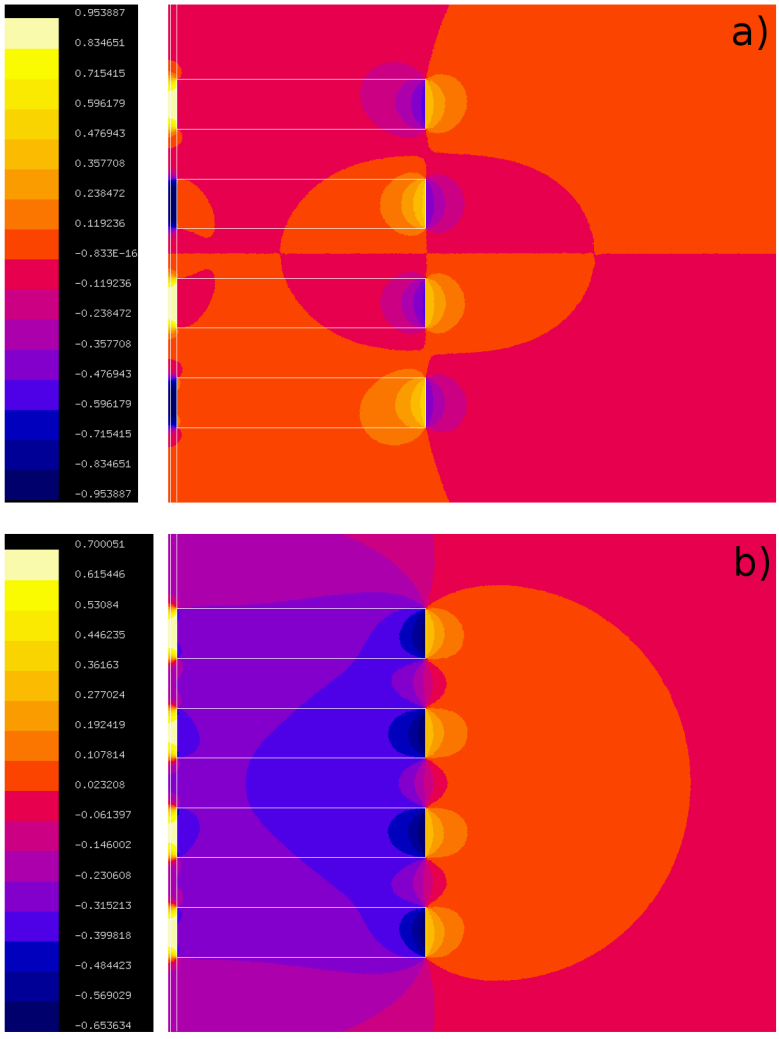

Figure S 7: Isovalue representation of the x component of the magnetic flux density in a) repulsion and b) attraction.

$\boldsymbol{B_0}$ *= 1T,* $\Delta r_{mag}/t$ *= 5,* t *= 2 mm and* r_{ext} *= 187.5 µm*

SI 7: Saturation magnetization (attraction configuration)

The (A) curve of Fig.S8 presents the *x*-component of the magnetic force with four magnets in attraction. This component has a positive value on the left and a negative one on the right of every magnet (shaded), concentrating the beads towards the middle of the magnet. Three additional inter-magnet plugs with a smaller force are present. Logically the magnetic force maxima decrease with $\boldsymbol{B_{sat}}$, but the number of MBs plugs and their position remain the same. When $\boldsymbol{B_{sat}}$ passes from 1 T (corresponding to $\boldsymbol{B}$ imposed in the magnets) to 0.1 T, the magnetic force's loss is 4 times in attraction. Indeed, in this configuration, the magnetic flux density is lower inside the magnet borders than in repulsion. Moreover, the magnetic force maxima are not located at the magnetic flux density maxima, minimizing the loss when varying $\boldsymbol{B_{sat}}$. When considering a $\boldsymbol{B_{sat}}$ of 0.1 T, the magnetic force in repulsion and attraction has a similar magnitude, slightly above 100 pN.

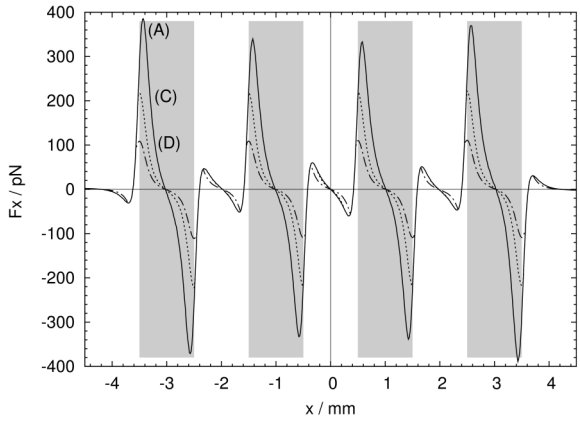

Figure S 8: Variation of the magnetic force (x component) for four magnets in) attraction, for several saturation magnetic flux density B_{sat}. (A) 1 T, (C) 0.2 T and (D) 0.1 T. The forces were calculated for a bead of radius = 500 nm and B_0 = 1 T. $r_{mag.int}$ = 187.5 µm, Δr_{mag} = 5 mm, t =1 mm and d = 1mm. All the values are taken along the x-axis. The grey surfaces show the position of the four magnets.

SI 8: Concentration isovalues in function of the apparent diffusion coefficient

The apparent diffusion coefficient D, representing the repulsion between beads columns, was estimated by comparing the concentration isovalues presented below with the experimental visualizations in Fig. 5 of the paper. As the apparent diffusion coefficient increases, the plugs become larger, canceling their parabolic shape given by the flow, and the concentration of the MBs decreases. A value of $4 \cdot 10^{-8}$ m^2/s was chosen.

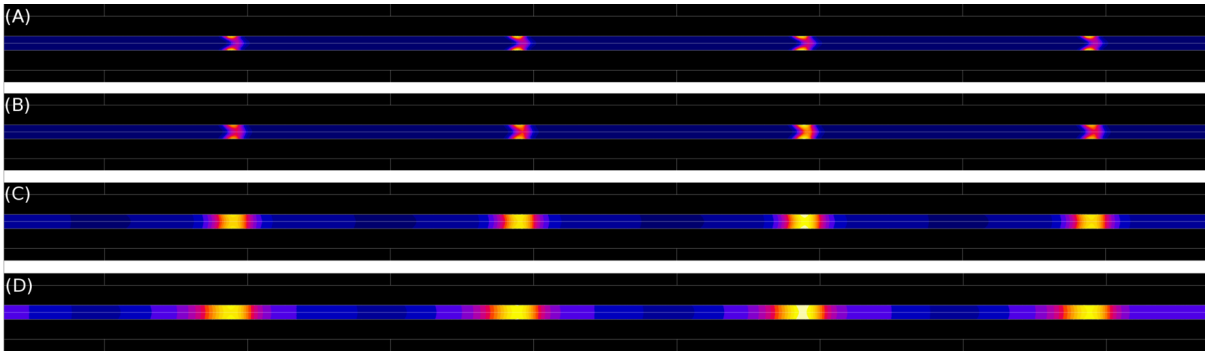

Figure S 9: Isovalue representation of MBs concentration, at a flow mean velocity of 1 mm/s in repulsion configuration, as a function of the apparent diffusion coefficient D. (A) $5 \cdot 10^{-9}$ m^2/s, (B) $1 \cdot 10^{-8}$ m^2/s, (C) $5 \cdot 10^{-8}$ m^2/s and (D) $1 \cdot 10^{-7}$ m^2/s. The maximum c value is (A) 584.18 mM, (B) 260.99 mM, (C) 11.57 mM and (D) 5.24 mM. Bead radius = 150 nm and B_0 = 1.3 T.

SI 9: Comparison of 2D and axisymmetrical simulations

Numerical simulations in 2D were carried out to complete the axisymmetrical ones. Four magnets in series were taken into account and the magnetic force was calculated for a saturation magnetic flux density B_{sat} of 0.1 T, in both repulsion and attraction configurations. Figure S10 shows the comparison between axisymmetrical and 2D simulations in repulsion. It can be seen that the number and position of maxima is the same. The force is higher in the axisymmetrical case, because of a higher gradient of $\boldsymbol{B}$.

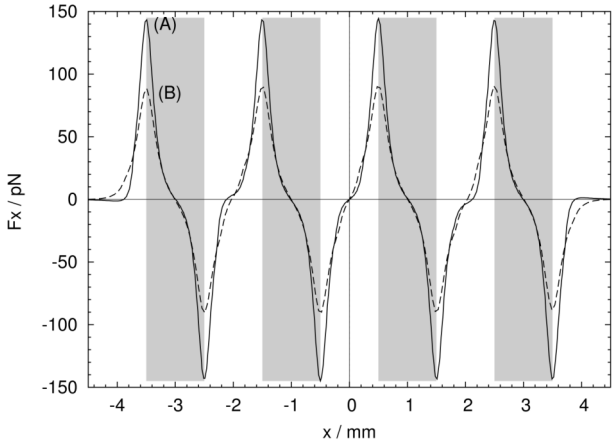

Figure S 10: Magnetic force (x component) for four magnets in repulsion. (A) axisymmetrical simulation and (B) 2D simulation. The forces were calculated for the following parameters: $\boldsymbol{B_0}$ *= 1.3 T,* Δr_{mag} *= 5 mm, t = 1 mm,* $r_{mag.int}$ *= 187.5 μm, r = 500 nm and* χ *= 1. The grey surfaces show the position of the four magnets.*

In attraction, as shown in Figure S11, the number and position of the peaks is the same for both curves. Again the magnetic force is lower in the 2D case for the reasons previously mentioned. The inter-magnet forces are nearly negligible in 2D, but nevertheless the tendency is the same, enabling the extrapolation of a 3D case, which would be between these two extreme situations.

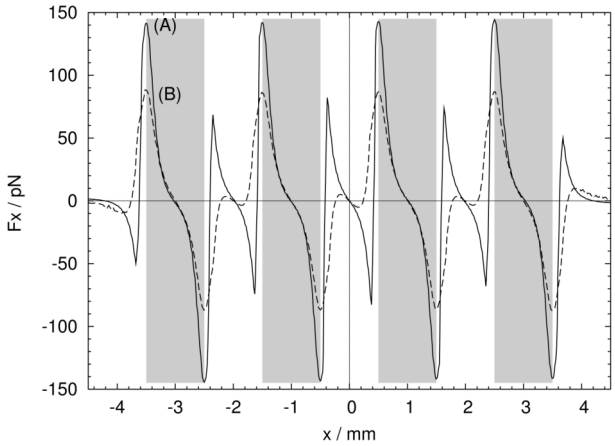

Figure S 11: Magnetic force (x component) for four magnets in attraction. (A) axisymmetrical simulation and (B) 2D simulation. The forces were calculated for the following parameters: $\boldsymbol{B_0}$ *= 1.3 T,* Δr_{mag} *= 5 mm, t = 1 mm,* $r_{mag.int}$ *= 187.5 μm, r = 500 nm and* χ *= 1. The grey surfaces show the position of the four magnets.*